coatings

MDPI

Article

Effect of Shellac Microcapsules Blended with Carbonyl Iron Powder and Carbon Nanotubes on the Self-Healing and Electromagnetic Wave Absorption Properties of Waterborne Coatings on Fiberboard Surface

Yongxin Xia [1,2], Wenbo Li [1,2] and Xiaoxing Yan [1,2,*]

[1] Co-Innovation Center of Efficient Processing and Utilization of Forest Resources, Nanjing Forestry University, Nanjing 210037, China; xiayongxin@njfu.edu.cn (Y.X.); liwenbo@njfu.edu.cn (W.L.)
[2] College of Furnishings and Industrial Design, Nanjing Forestry University, Nanjing 210037, China
* Correspondence: yanxiaoxing@njfu.edu.cn

Abstract: An orthogonal experiment was conducted to prepare nine different coatings by changing four influencing factors of shellac microcapsule content, carbonyl iron powder (CIP) content, the content of carbon nanotubes (CNTs), and primer coating thickness. By testing the morphology and performance of the shellac microcapsules, CIP, CNT blended coatings (SCCBC), and using the elongation at tensile failure of the SCCBC as the orthogonal experimental analysis, it was determined that the biggest factor affecting the elongation at tensile failure of SCCBC was the shellac microcapsule content. With the aim of further optimizing the properties of the SCCBC, a single-factor experiment was performed using shellac microcapsule content as the sole variable, and it was determined that the SCCBC exhibited optimal performance when shellac microcapsule content reaches 4.2%. The optical properties of SCCBC were tested, showing that there were minor fluctuations in the glossiness and color difference of the SCCBC. The mechanical properties of SCCBC were tested. The presence of shellac microcapsules can contribute to an improvement of the SCCBC toughness, restraining the formation of microcracks, and have a certain self-healing effect. The electromagnetic wave absorption properties of the mixed powder of shellac microcapsules, CIP and CNTs were tested. The CIP and CNTs can enhance the electromagnetic wave absorption properties of the waterborne coating, but the electromagnetic wave absorption properties were weaker in low-frequency bands. The SCCBC on the surface of fiberboard not only have a self-healing effect, but also have a certain electromagnetic wave absorption function through the mixing of shellac microcapsules, CIP, and CNTs, expanding the application range of waterborne coatings for wood.

Keywords: microcapsules; waterborne coatings; electromagnetic wave absorption; self-healing

Citation: Xia, Y.; Li, W.; Yan, X. Effect of Shellac Microcapsules Blended with Carbonyl Iron Powder and Carbon Nanotubes on the Self-Healing and Electromagnetic Wave Absorption Properties of Waterborne Coatings on Fiberboard Surface. *Coatings* **2023**, *13*, 1572. https://doi.org/10.3390/coatings13091572

Academic Editor: Alina Vladescu

Received: 14 August 2023
Revised: 4 September 2023
Accepted: 6 September 2023
Published: 8 September 2023

1. Introduction

Waterborne coatings are abrasion resistant and non-toxic, providing protection for wooden furniture. However, the waterborne coatings will be damaged by external factors during use, resulting in microcracks [1–6]. Self-healing microcapsules can have a certain inhibitory effect on microcracks in waterborne coatings [7–11]. A melamine resin is non-toxic and odorless, with a simple preparation process and compact material, making it a good choice for microcapsule wall materials. As a natural material, shellac has the characteristics of fast drying, strong adhesion, and high hardness. Applying the shellac as a microcapsule core material to waterborne coatings on wood surfaces can effectively protect the wooden substrates [12–14]. The shellac microcapsules prepared with the rosin-modified yellow shellac solution have good self-healing, mechanical, and optical properties.

Electromagnetic wave absorption materials of the coating type can change their absorbency by adjusting the amount of absorbing powder added to the coating. This method

is widely used due to its simple operation, strong material adaptability, low cost, and better effect. The carbonyl iron powder (CIP) has benefits of high electromagnetic loss, absorption frequency bandwidth, and low price, making it widely used in the domain of absorption. However, as a result of its high density, its impedance matching performance is poor, which affects its electromagnetic wave absorption performance [15–19]. The carbon nanotubes (CNTs) have the advantages of absorbing frequency bandwidth, light weight, and good electromagnetic shielding performance [20,21]. Mixing CIP with CNTs can not only improve the shortcomings of poor impedance matching performance and high density of CIP, but also enhance the absorbing performance [22,23].

The shellac microcapsules were used as the coating repair agent and blended with CIP and CNTs. The waterborne coatings were prepared on the surface of fiberboard substrate through orthogonal experiments. The results of the orthogonal experiments were analyzed, and further single-factor experiments were conducted to prepare an electromagnetic absorbing coating with self-healing performance. The waterborne coatings on the fiberboard surface not only have a self-healing effect but also have a certain absorbing function, expanding the application range of waterborne coatings for wooden materials. Applying the self-healing and electromagnetic wave absorption of dual-function coatings to the surface of wooden materials reduces the impact of electromagnetic radiation on human bodies in daily life and improves people's living environments. The results offer a guidance for applying dual-function coatings with self-healing and electromagnetic absorption capabilities on the surface of wooden materials.

2. Experimental Materials and Methods

2.1. Experimental Materials and Instruments

The materials used in this paper are detailed in Table S1. Table S2 shows the experimental instruments.

2.2. Preparation of Shellac Microcapsules, CIP, CNT Blended Coatings (SCCBC)

2.2.1. Preparation of Shellac Microcapsules

The microcapsules used in the experiment are shellac microcapsules with a wall to core ratio of 1:0.80 [24]. The specific preparation process is referred to the research by Li [25].

2.2.2. Preparation of Shellac Microcapsules, CIP, CNT Blended Powders

Firstly, the CIP was placed in ethanol and ultrasonically agitated for 10 min. Then, CIP was attracted by a strong magnet, and anhydrous ethanol and deionized water were used to clean the CIP. After drying, the CIP with impurities removed was obtained [26]. Sodium dodecyl benzene sulfonate was added to deionized water at a mass fraction of 0.1% as an emulsifier. After the sodium dodecyl benzene sulfonate was completely dissolved, the shellac microcapsules, CIP, and CNTs were added to the emulsifier in corresponding amounts. After being sonicated for one hour, the solution was placed to a constant temperature oven at 60 °C until the water evaporates completely. The dried blended material was ground into powder to obtain the required shellac microcapsules, CIP, CNT blended powder.

2.2.3. Preparation of SCCBC on the Fiberboard

The L_9 (3^4) orthogonal experiment was designed with content of shellac microcapsules, CIP content, CNTs content, and primer coating thickness as the factors. The orthogonal experimental factors and levels are detailed in Table 1. The orthogonal experimental arrangement is detailed in Table 2, and the materials utilized for the orthogonal experiment are detailed in Table 3. The # indicates the sample number unit. The powder was added to the waterborne primer according to different content ratios, and the total amount of primer was controlled to 4.00 g. According to Table 2, the SZQ four-sided coating preparation machine was used to coat the primer on the fiberboard according to the required thickness

of the waterborne primer. After drying for 24.0 h, the waterborne topcoat was treated in the same way without adding powder, and the total thickness of the SCCBC were maintained at 60 μm. After allowing the mixture to cure for 24.0 h, the mechanical, optical, and liquid resistance properties of SCCBC on fiberboard surface were tested.

Table 1. Orthogonal experimental factors and levels.

Level	Addition Amount of Shellac Microcapsules (%)	Addition Amount of CIP (%)	Addition Amount of CNTs (%)	Primer Coating Thickness (μm)
1	2.0	10.0	0	10
2	4.0	20.0	1.0	20
3	6.0	40.0	2.0	25

Table 2. Orthogonal experiment schedule.

Sample (#)	Addition Amount of Shellac Microcapsules (%)	Addition Amount of CIP (%)	Addition Amount of CNTs (%)	Primer Coating Thickness (μm)
1	2.0	10.0	0	10
2	2.0	20.0	1.0	20
3	2.0	40.0	2.0	25
4	4.0	10.0	1.0	25
5	4.0	20.0	2.0	10
6	4.0	40.0	0.0	20
7	6.0	10.0	2.0	20
8	6.0	20.0	0.0	25
9	6.0	40.0	1.0	10

Table 3. Materials for orthogonal experiments.

Sample (#)	Shellac Microcapsules (g)	CIP (g)	CNTs (g)	Deionized Water (g)	Sodium Dodecyl Benzene Sulfonate (g)	Primer (g)
1	0.08	0.40	0	23.50	0.02	3.52
2	0.08	0.80	0.04	45.04	0.04	3.08
3	0.08	1.60	0.08	86.16	0.08	2.24
4	0.16	0.40	0.04	29.37	0.03	3.40
5	0.16	0.80	0.08	50.91	0.05	2.96
6	0.16	1.60	0	86.16	0.08	2.24
7	0.24	0.40	0.08	35.25	0.03	3.28
8	0.24	0.80	0	50.91	0.05	2.96
9	0.24	1.60	0.04	92.03	0.09	2.12

2.2.4. Preparation of SCCBC on the Glass Slide

The powder was added to the waterborne primer according to different content ratios. The total amount of primer was controlled to 4.00 g, and it was stirred evenly. The SZQ four-sided coating preparation machine (Table S2) was used to coat the primer on the glass slide according to the required thickness of the primer. After drying for 24.0 h, the topcoat was treated in the same way without adding powder, and the total thickness of the SCCBC was maintained at 60 μm. After allowing the mixture to cure for 24.0 h, the SCCBC were slowly scraped away by the blade, and the self-healing and elongation at the tensile failure rate were tested.

In accordance with the experimental process described above, a single-factor experiment was conducted, varying shellac microcapsule content at quantities of 3.0%, 3.4%, 3.8%, 4.2%, 4.6%, 5.0%, and 5.4%, respectively. The material for the single-factor experiment is detailed in Table 4.

Table 4. Material for a single-factor experiment.

Content of Shellac Microcapsules (%)	Shellac Microcapsules (g)	CIP (g)	CNTs (g)	Water (g)	Sodium Dodecyl Benzene Sulfonate (g)	Primer (g)
3.0	0.12	0.80	0.08	48.95	0.05	3.00
3.4	0.13	0.80	0.08	49.44	0.05	2.99
3.8	0.15	0.80	0.08	50.42	0.05	2.97
4.2	0.17	0.80	0.08	51.44	0.05	2.95
4.6	0.18	0.80	0.08	52.95	0.05	2.94
5.0	0.20	0.80	0.08	53.95	0.05	2.92
5.4	0.22	0.80	0.08	54.94	0.06	2.90

2.3. Testing and Characterisation

2.3.1. Microscopic Characterization

Scanning Electron Microscope (Table S2): The SCCBC were glued onto the sample tray for gold spraying and vacuum pumping operations. The SCCBC were observed when the vacuum is below 3 KPa.

2.3.2. Chemical Composition

The infrared spectrometer with an attenuated total reflection device was employed to test the chemical constituent of the SCCBC. The SCCBC were placed on the observation stage to facilitate the testing process.

2.3.3. Optical Properties

The color difference of the SCCBC was tested by the 3nhYS3010 color difference instrument. The sample was observed under directional observation CIE10°, directional illumination 45°, and standard illumination D_{65} field of view. The color difference instrument was placed in two different positions on the SCCBC to record the L_1, a_1, b_1 values and L_2, a_2, b_2 values. The color difference ΔE between two positions was calculated according to the CIELAB color difference formula, as shown in formula (1), where $\Delta L = L_1 - L_2$, $\Delta a = a_1 - a_2$, $\Delta b = b_1 - b_2$. Among them, the L represents the brightness value of the SCCBC, with a higher L value indicating a brighter SCCBC. The a represents the red–green chromaticity value of the SCCBC; a higher value of a indicates a redder SCCBC and a vice versa for greener SCCBC. The b represents the yellow–blue chromaticity value of the SCCBC; a higher b value indicates a yellower SCCBC and a vice versa for bluer SCCBC.

$$\Delta E = [(\Delta L)^2 + (\Delta a)^2 + (\Delta b)^2]^{1/2} \quad (1)$$

The glossiness of the SCCBC were tested using a 3nhYG60S glossmeter at 20°, 60°, and 85° incidence angles. According to the standard, the glossiness at 60° incidence angle is applicable to all coatings. Therefore, the glossiness value at 60° incidence angle was selected for analysis of the SCCBC glossiness [27].

2.3.4. Mechanical Properties

The adhesion of the SCCBC were tested by the QFH-A coating adhesion tester. Firstly, the cutting tool was positioned vertically against the surface of the SCCBC, and it was uniformly drawn at an appropriate distance. All cutting should slide through to the surface of the substrate. Then, an equal number of parallel cutting lines intersecting at a 90° angle to the original cutting lines were created, forming a grid. The adhesive strip was used to paste flat above the grid, and the falling off of the coating after tearing was observed. The adhesion of the coating is categorized into six levels: 0, 1, 2, 3, 4, and 5, which correspond to the detachment areas of 0%, <5%, <15%, <35%, <65%, and >65%, respectively.

The hardness of the SCCBC were tested by the HT-6510P pencil hardness tester. The 9B-9H pencils were chosen from soft to hard. The pencil which was trimmed around 5 mm of wood from the end was inserted into the apparatus, with the pencil tip aligned parallel

to the coating surface, and it was pushed smoothly for a distance of at least 7 mm at a velocity of approximately 0.5 mm/s. The pencil hardness was the maximum hardness of the SCCBC when the SCCBC surface remains unharmed.

The impact resistance of the SCCBC were tested by the QCJ-40 coating impactor (Table S2). The SCCBC was laid on a level base. The impactor was positioned above the SCCBC, and the steel ball was centered at the impact location. The impactor was elevated to a predetermined impact height, and then allowed to descend. Then, the SCCBC were exposed to natural light, and the cracking of the SCCBC were examined using a magnifying glass. When there is no occurrence of cracking or peeling in the SCCBC, the maximum height attained represents the maximum impact resistance height.

Parallel to direction of coating elongation, the blade was used to create cracks on the SCCBC. Mechanical tensile tests on three variations in coatings (unaltered SCCBC, scratched SCCBC, and repaired SCCBC after 24.0 h) were performed using a universal mechanical testing machine. Formula (2) is utilized to calculate the elongation at tensile failure of the SCCBC in different states, which is used to demonstrate the repair result of the SCCBC. The self-healing rate of the SCCBC was calculated according to formula (3) [28].

$$E = [(L_h - L_0)/L_0] \times 100\% \quad (2)$$

Among them: E is the elongation at tensile failure of the SCCBC; L_h is the length of the standard line measured by assembling the broken SCCBC; L_0 is the initial length of the SCCBC.

$$\eta = [(E_H - E_S)/(E_I - E_S)] \times 100\% \quad (3)$$

Among them: η is the self-healing rate of the SCCBC; E_H is the elongation at tensile failure of the SCCBC after 24.0 h of repair; E_S is the elongation at tensile failure of the SCCBC following scratching; E_I is the elongation at tensile failure of the original SCCBC.

2.3.5. Roughness

The SCCBC were placed on the experimental table, and coating roughness measurements were conducted by gradually moving a diamond-tipped probe with a curvature radius of approximately 2 μm across the surface. R_a represents the arithmetic average roughness and the R_a value is the roughness of the SCCBC.

2.3.6. Liquid Resistance

A 75% ethanol aqueous solution, red ink solution, dishwashing liquid, and 15% NaCl solution were selected to perform liquid resistance tests on the SCCBC. The 75% ethanol aqueous solution represents neutral fluids, the red ink solution signifies more heavily colored fluids, the dishwashing liquid symbolizes everyday products, and the 15% NaCl solution represents alkaline fluids. These four items encompass the majority of liquid types that furniture could encounter during its regular usage. In the course of preparation, four pliable filter paper sheets were submerged in their corresponding testing solutions for a span of approximately 30 s. Then, these sheets were positioned onto the surface of the SCCBC, and extracted following a duration of 24.0 h. Surplus solution was then eliminated from the surface, and the extent of damage within the test area was scrutinized. The assessment to determine the liquid resistance level was performed. The liquid resistance level is categorized into levels 1 to 5, with the evaluation standard elucidated in Table 5. The color difference and glossiness of the experimental area were simultaneously observed.

Table 5. Evaluation standard for liquid resistance level of SCCBC.

Liquid Resistance Level	Standard
1	No modification is observed in the coating.
2	A slight change in color becomes visible as the light source moves nearer.
3	There are slight marks that can be observed.
4	The imprints are quite severe, but the overall structure and appearance of the coating remains unchanged.
5	Severe imprinting, changes in material structure, such as blistering, cracking.

2.3.7. Electromagnetic Wave Absorption Performance

The electromagnetic properties of the prepared samples were evaluated by employing the Agilent E8363C vector network analyzer (Table S2). Theoretical reflection loss (RL) of the samples was computed utilizing a transmission line theory. A decrease in theoretical reflection loss values signifies an enhanced absorption performance of the material. The electromagnetic wave absorption performance test was conducted on the shellac microcapsules, CIP, CNT blended powders.

All tests mentioned above were repeated on four times, and the error was less than 5.0%.

3. Results and Discussion

3.1. Analysis of Orthogonal Experimental Results

The elongation at tensile failure of a coating refers to the degree to which a coating can deform and stretch under a tensile action. It represents the ductility of the coating and is a significant indicator of the tensile and fracture resistance of coating. Therefore, the elongation at tensile failure of the coating is taken as the orthogonal experimental result. In orthogonal experiments, a range is an indicator used to evaluate the degree of change in experimental results caused by different factors. Specifically, each factor in the orthogonal experimental design has multiple levels, and each level corresponds to a mean. The difference between different means represents the average impact of different factors on the experimental results. The larger the disparity in means among various factors, the more pronounced the influence of that factor on the trial outcomes. Conversely, the smaller the difference between the mean values of different factors, the less the impact of the factor on the experimental results. The range analysis of the elongation at tensile failure of the SCCBC is shown in Table 6, and the effect curve of the elongation at tensile failure is detailed in Figure 1. The analysis of the range of results reveals that shellac microcapsule content has the greatest impact on the elongation at tensile failure of the SCCBC, followed by the content of CNTs. The content of CIP and the thickness of the primer coating have a smaller impact. According to the variance analysis of the elongation at tensile failure of the SCCBC, the results of the variance analysis for the four factors mentioned above are compliant with the range analysis results. Combining the mean range values in Figure 1 and Table 6, it can be concluded that the elongation at tensile failure of the SCCBC is better when the CIP content is 20.0%, the CNTs content is 2.0%, and the primer coating thickness is 25 μm. Therefore, the CIP content was determined to be 20.0%, the CNTs content to be 2.0%, and the thickness of the primer coating to be 25 μm. The surface changes in the fiberboard before and after coating are detailed in Figure 2.

Table 6. Analysis of range of the elongation at tensile failure of the SCCBC.

SCCBC	Shellac Microcapsules (%)	CIP (%)	CNTs (%)	Primer Coating Thickness (μm)	Elongation at Tensile Failure (%)
1 #	2.0	10.0	0	10	0.3
2 #	2.0	20.0	1.0	20	1.0
3 #	2.0	40.0	2.0	25	1.6
4 #	4.0	10.0	1.0	25	1.8
5 #	4.0	20.0	2.0	10	2.6
6 #	4.0	40.0	0	20	1.5
7 #	6.0	10.0	2.0	20	1.4
8 #	6.0	20.0	0	25	1.6
9 #	6.0	40.0	1.0	10	1.0
mean value 1	0.992	1.183	1.125	1.317	
mean value 2	1.958	1.717	1.292	1.317	
mean value 3	1.342	1.392	1.875	1.658	
Range	0.966	0.534	0.750	0.341	
DEVSQ	1.536	0.496	0.916	0.269	
degrees of freedom	2	2	2	2	
F ratio	1.910	0.617	1.139	0.334	
F critical value	4.460	4.460	4.460	4.460	
significance					

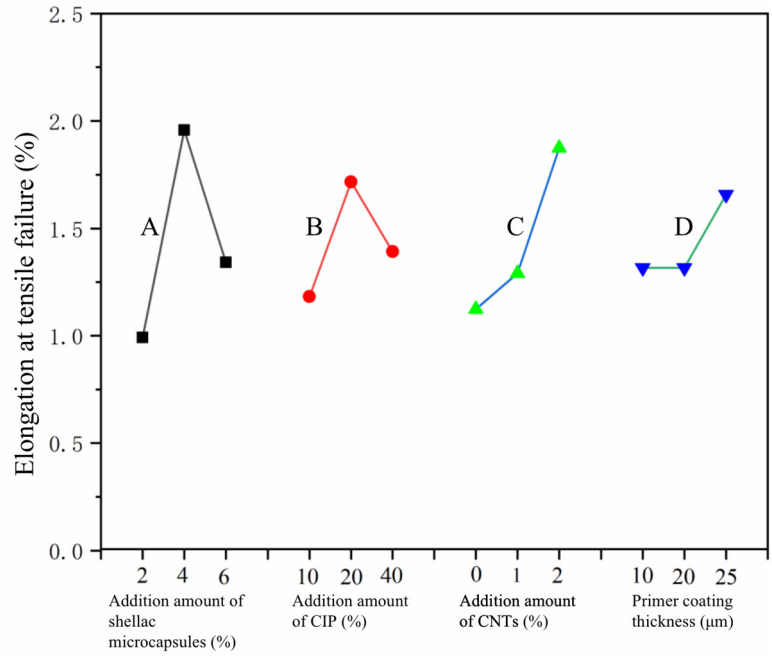

Figure 1. Elongation at tensile failure effect curve: (A) addition amount of shellac microcapsules, (B) addition amount of CIP, (C) addition amount of CNTs, and (D) primer coating thickness.

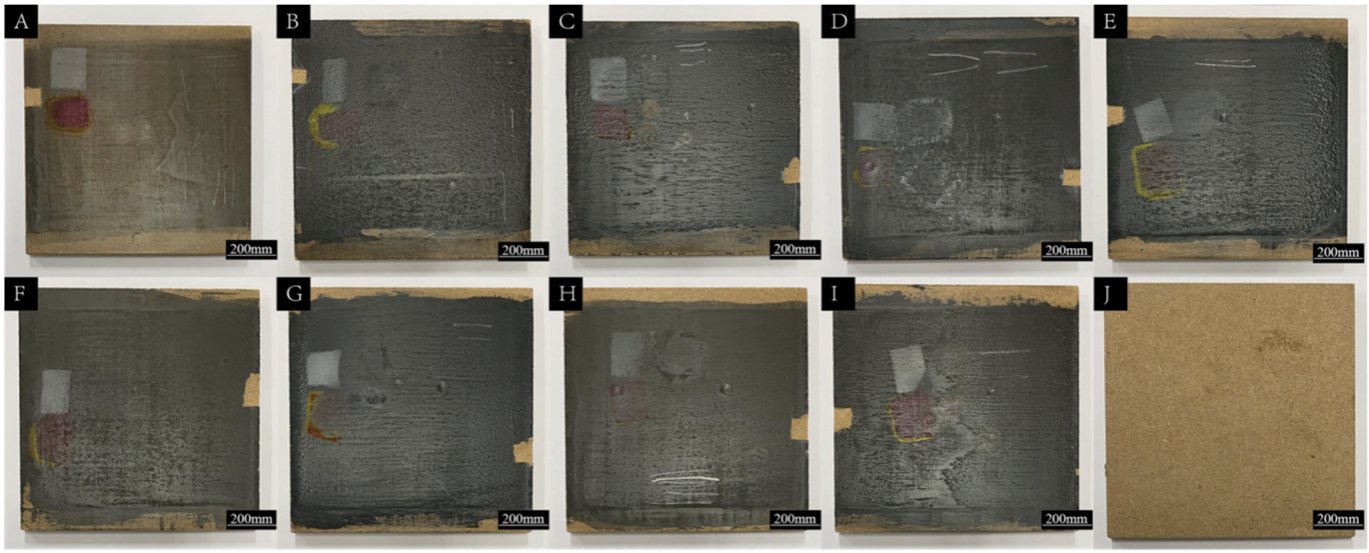

Figure 2. Surface changes in the fiberboard before and after coating: (**A**–**I**) 1–9 #; (**J**) untreated fiberboard.

3.2. Analysis of Optical Properties of SCCBC

Measuring two different positions of the same sample indirectly measures whether the dispersion of microcapsules in the SCCBC is uniform by comparing the color differences between the two positions. The chromaticity values and color differences of the SCCBC are detailed in Table 7. With the increasing amount of shellac microcapsules added, the SCCBC exhibits an incremental rise in color difference, but the overall change is not significant. This is because CIP and CNTs are both black, and when blended with the coating, the color of the SCCBC appears black. Changing the content of CIP and CNTs, the degree of black change in the SCCBC is still not significant, thus having a small impact on color difference. The color difference of the SCCBC remains nearly unaffected when the amount of shellac microcapsules is below 4.2%. When the amount of shellac microcapsules added is 5.4%, the maximum color difference reaches 2.08. The reason may be that when there is an excessive amount of shellac microcapsules, the relative content of shellac microcapsules, CIP, CNTs blended powders in the waterborne primer increases, and it cannot be uniformly dispersed in the waterborne coating, resulting in a small amount of aggregation, which increases the color difference [29–31].

Table 7. Chromaticity value and color difference of SCCBC.

Content of Shellac Microcapsules (%)	L_1	a_1	b_1	L_2	a_2	b_2	ΔL	Δa	Δb	ΔE
0	49.60	9.12	25.32	49.65	9.19	25.6	−0.05	−0.07	−0.28	0.29
3.0	25.31	0.95	1.83	24.87	1.52	1.64	0.44	−0.57	0.19	0.74
3.4	24.07	1.01	1.79	23.98	0.65	0.96	0.09	0.36	0.83	0.91
3.8	22.30	−0.29	0.45	23.07	0.58	0.79	−0.77	−0.87	−0.34	1.21
4.2	21.35	0.66	0.62	20.23	0.31	0.15	1.12	0.35	0.47	1.26
4.6	19.33	0.38	0.13	20.87	0.96	0.78	−1.54	−0.58	−0.65	1.77
5.0	20.58	−0.16	0.84	18.87	0.46	0.43	1.71	−0.62	0.41	1.85
5.4	18.09	0.75	0.35	19.83	−0.26	0.88	−1.74	1.01	−0.53	2.08

The glossiness values of the SCCBC are detailed in Table 8. With the increasing amount of shellac microcapsule content, the SCCBC exhibits an incremental decrease in glossiness. When the shellac microcapsule content is between 3.0% and 4.2%, the glossiness of the SCCBC hardly changes. However, when it surpasses 4.2%, the glossiness of the SCCBC decreases significantly, with a minimum of 18.6 GU. This is because shellac microcapsules are a solid powder. With the rising quantity of shellac microcapsules, the powder in the

SCCBC also increases. This change impacts the surface smoothness and mirror reflection capability of the SCCBC, leading to a gradual reduction in glossiness as shellac microcapsule content rises [32].

Table 8. Glossiness values of SCCBC with different microcapsule contents.

Content of Shellac Microcapsules (%)	20° Glossiness Value (GU)	60° Glossiness Value (GU)	85° Glossiness Value (GU)
0	20.5	50.1	52.4
3.0	19.4	46.4	49.1
3.4	18.3	44.3	48.6
3.8	17.3	44.4	49.8
4.2	13.9	37.8	45.3
4.6	6.4	23.2	29.1
5.0	4.9	20.2	25.1
5.4	4.3	18.6	23.6

3.3. Analysis of Mechanical Properties and Roughness of SCCBC

The mechanical properties and roughness of the SCCBC are detailed in Table 9. The adhesion level of the SCCBC gradually increases with the rising quantity of shellac microcapsules, indicating a gradual decrease in the adhesion of the SCCBC. The reason for this is the inclusion of powder in the primer. With a gradual rise in powder content, the SCCBC experiences an increase in particulate matter. Consequently, this affects the adhesion capability between the SCCBC and the wooden substrate, resulting in a reduction in the adhesion of the SCCBC. When the content of shellac microcapsules is below 4.2%, the SCCBC adhesion level is 1–2, which is slightly worse than the adhesion ability in previous research results [33], but has little impact on the SCCBC. The hardness of the SCCBC gradually rises with the increasing amount of powder content, reaching a maximum of 4H. The shellac microcapsules have a certain volume and shape, and adding them to waterborne coatings can fill the gaps and pores in the coating matrix. The addition of shellac microcapsules increases the solid content of coatings, thereby increasing the density of the coating and gradually increasing the hardness of the SCCBC [34]. As the powder content increases, the impact resistance of the SCCBC follows a pattern of first rising and then declining. When the shellac microcapsule content reached 4.2%, the impact resistance of the SCCBC was the highest, reaching 15 kg·cm. By comparison with the coating without microcapsules, the impact resistance is significantly enhanced. This is because adding shellac microcapsules can increase the hardness of the SCCBC, but the toughness of the SCCBC decreases, making it prone to cracks under external impact, resulting in a decrease in the impact resistance of the SCCBC [35]. The change in roughness of SCCBC with different microcapsule contents is detailed in Figure 3. The roughness of the SCCBC gradually increases with the increase in shellac microcapsule content. The shellac microcapsules are powders, and an increase in the content of shellac microcapsules in the coating will inevitably affect the smoothness of the coating surface, leading to an increase in SCCBC roughness.

Table 9. Mechanical properties and roughness of SCCBC.

Content of Shellac Microcapsules (%)	Adhesion (Degree)	Hardness	Impact Resistance (kg·cm)	Roughness (μm)
0	1	H	6	0.489
3.0	1	H	7	2.151
3.4	1	H	9	2.365
3.8	2	2H	11	2.564
4.2	2	2H	15	2.593
4.6	3	3H	13	2.826
5.0	4	3H	12	3.024
5.4	4	4H	9	3.125

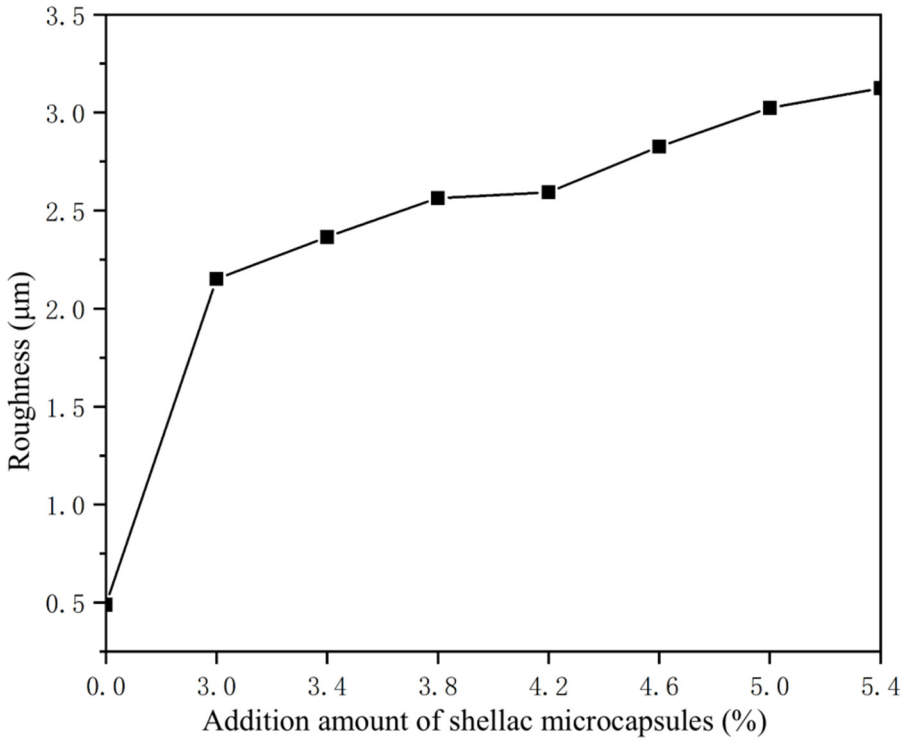

Figure 3. Change in roughness of SCCBC with different shellac microcapsule contents.

3.4. Analysis of the Elongation at Tensile Failure and the Self-Healing Rate of SCCBC

The results of the elongation at tensile failure of the SCCBC are detailed in Table 10. The elongation at tensile failure of the original coating with the addition of shellac microcapsules is higher than that without the addition of microcapsules. This is because shellac has high strength viscosity and is elastic. Upon the occurrence of external factors causing damage to the coating, the wall material of the microcapsule ruptures, and shellac flows out to strengthen the toughness of the coating. Therefore, the addition of microcapsules can enhance the tensile resistance of the SCCBC [36]. When there is an excessive amount of shellac microcapsules, the elongation at tensile failure of the SCCBC gradually increases. When the amount of shellac microcapsules added reaches 4.2%, the elongation at tensile failure of the SCCBC reaches the maximum of 8.2%. As the amount of shellac microcapsules added further increases, the elongation at tensile failure of the SCCBC decreases gradually. This is due to the fact that an excessive content of shellac microcapsules leads to an increased proportion of powder in the coating. As a result, the dispersion of the powder within the coating becomes uneven, causing a reduction in the toughness of the SCCBC and making it more prone to becoming brittle and fracturing. According to formula (3), the self-healing rate of the SCCBC was calculated, and the coating without adding microcapsules does not have a repair effect. This is because when the coating produces scratches, the lack of repair agents in the coating further expands the microcracks under environmental influence. When the amount of microcapsules increased from 3.0% to 4.2%, the self-healing rate of the SCCBC increased by 11.6%. When the content of shellac microcapsules reaches 4.2%, the repair effect of the SCCBC was the best, reaching 24.1%. When the amount of shellac microcapsules increased from 4.2% to 5.4%, the self-healing rate of the SCCBC decreased by 12.6%. The reason for this is that when the content of shellac microcapsules is low, the shellac microcapsules can be evenly scattered in the SCCBC. When the SCCBC is damaged by external factors, the microcracks occur. In the meanwhile, the shellac core material flows out of the microcapsules and cures at room temperature, bridging the microcracks, which plays a positive role in suppressing and repairing the microcracks in the SCCBC. When shellac microcapsule content is too high, on the one hand, the toughness of the SCCBC itself decreases, which affects the repair effect of the shellac core material. On the other

hand, the high content of shellac microcapsules leads to uneven dispersion in the SCCBC, which can lead to inconsistent repair effects of the SCCBC. The excessive accumulation of shellac microcapsules in some areas may result in more repair, while the areas with less distribution of shellac microcapsules have reduced repair performance [37].

Table 10. Elongation at tensile failure and self-healing performance of SCCBC.

Content of Microcapsules (%)	Elongation at Tensile Failure (%)			Self-Healing Rate (%)
	Original Sample	After Scratching	After Repairing	
0	5.3	3.8	3.1	-
3.0	5.8	4.2	4.4	12.5
3.4	6.3	4.3	4.7	20.0
3.8	6.7	4.8	5.2	21.1
4.2	8.2	5.1	5.8	24.1
4.6	7.8	4.8	5.3	16.7
5.0	7.3	4.7	5.1	15.4
5.4	6.9	4.3	4.6	11.5

3.5. Analysis of Liquid Resistance of SCCBC

The liquid resistance levels of SCCBC with different contents of shellac microcapsules are detailed in Table 11. Figures 4 and 5 show the changes in color difference and glossiness of SCCBC with different shellac microcapsule contents following liquid resistance compared to the untreated sample. The liquid resistance grade of level 1 is attributed to the SCCBC in the presence of 75.0% ethanol solution, dishwashing liquid, and 15.0% NaCl solution, indicating that these three solutions have almost no effect on the SCCBC. The cold resistance level of the red ink solution was level 5, indicating that the red ink solution has the greatest damage to the SCCBC. This is because the red ink solution contains solvents such as alcohol and ether, which can damage the SCCBC, dissolve the SCCBC, and disperse in the solvent, causing varying degrees of infiltration of red ink solution. After the SCCBC were treated with 75.0% ethanol solution, dishwashing liquid, and 15.0% NaCl solution, the color difference changed within 6. The red ink solution had the most significant effect on the color difference of the SCCBC, indicating that the red ink solution caused serious damage to the SCCBC. For different solutions, the overall glossiness shows a gradually decreasing trend. Due to the presence of powder, the smoothness of the SCCBC is affected, resulting in a decrease in glossiness. Additionally, the SCCBC surface after liquid resistance testing exhibits imprints similar to those left after liquid drying, which also affects the glossiness of the SCCBC.

Table 11. Liquid resistance level of SCCBC with different microcapsule contents.

Content of Shellac Microcapsules (%)	Liquid Resistance (Level)			
	75.0% Ethanol Solution	Red Ink Solution	Dishwashing Liquid	15.0% NaCl Solution
0	1	4	1	1
3.0	1	4	1	1
3.4	1	4	1	1
3.8	1	4	1	1
4.2	1	5	1	1
4.6	1	5	1	1
5.0	1	5	1	1
5.4	1	5	1	1

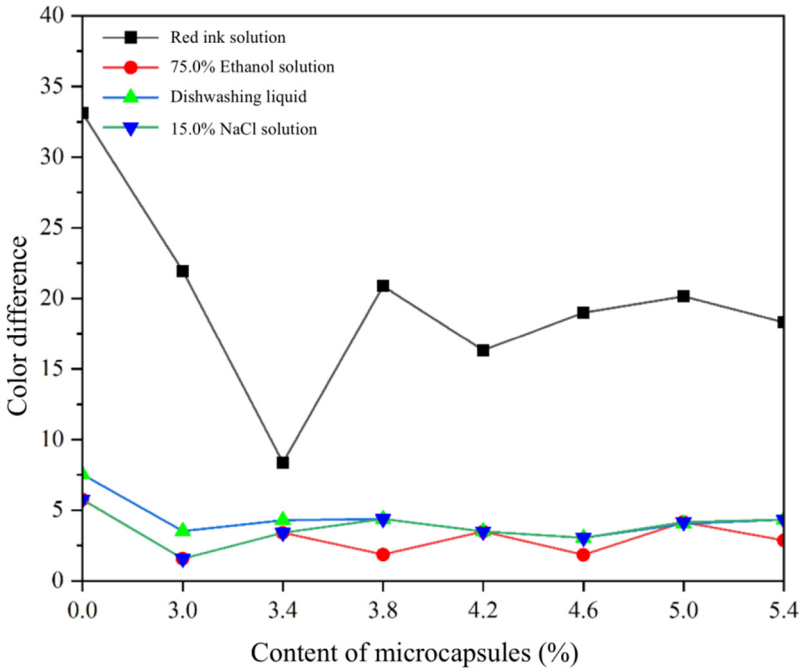

Figure 4. Changes in the color difference of SCCBC with different microcapsule content after liquid resistant tests.

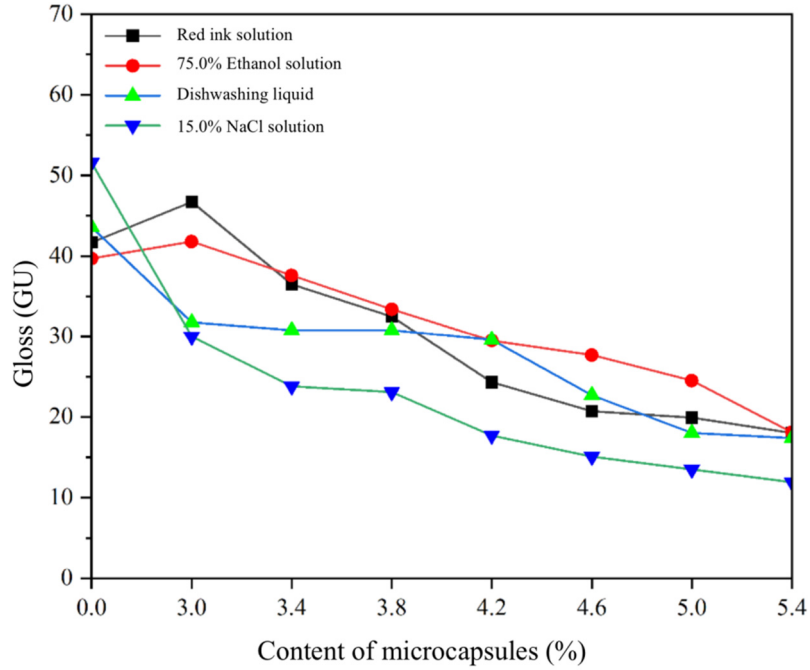

Figure 5. Changes in glossiness of SCCBC with different microcapsule content after liquid resistant tests.

3.6. Analysis of Microscopic Characterization of SCCBC

The microstructure of the SCCBC under different levels of shellac microcapsule content is detailed in Figure 6. There are some agglomeration phenomena on the surface of SCCBC with different levels of shellac microcapsules. This is because the microcapsules themselves are small particles, and the dispersion of CIP and CNTs in waterborne coatings is poor. As shellac microcapsule content increases, the surface agglomeration of the coating becomes more obvious. The surface of the coating with added 4.6% shellac microcapsules becomes more uneven, and the impact on the appearance and smoothness of the SCCBC increases.

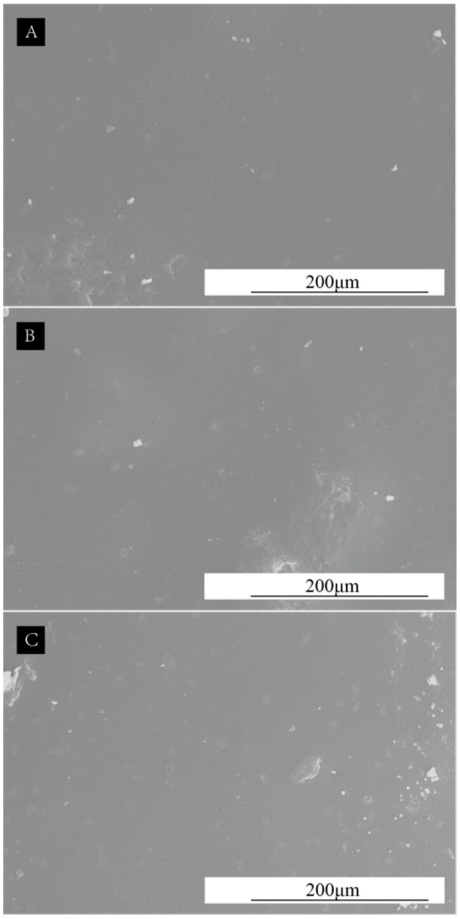

Figure 6. SEM image of SCCBC surface with different shellac microcapsule contents: (**A**) 3.8%, (**B**) 4.2%, and (**C**) 4.6%.

3.7. Infrared Analysis of SCCBC

As can be seen from Figure 7, the absorption peak at 1547 cm^{-1} is attributed to the stretching vibration of -NH-, and the appearance of the peak at 813 cm^{-1} corresponds to the bending vibration of the triazine ring, characteristic of melamine resin. This confirms the successful preparation of melamine resin. Shellac, as an animal resin, is a natural polymer with functional groups such as -OH, -COOH, and -COOC in its molecular structure. The absorption peaks at 2870 cm^{-1} and 2929 cm^{-1} are ascribed to the stretching vibration of C-H bonds in methyl ($-CH_3$) and methylene ($-CH_2-$) groups. The sharp peak at 1725 cm^{-1} corresponds to the stretching vibration of C=O bonds in polyester. The absorption peak at 3357 cm^{-1} is indicative of the stretching vibration of free hydroxyl (-OH) groups, while the range between 1620 cm^{-1} and 1450 cm^{-1} represents the skeletal stretching vibrations of benzene rings [38]. After conducting an analysis of these findings, it can be inferred that the inclusion of the shellac microcapsules, CIP, CNT blended powders has no impact on the original chemical composition of the coating.

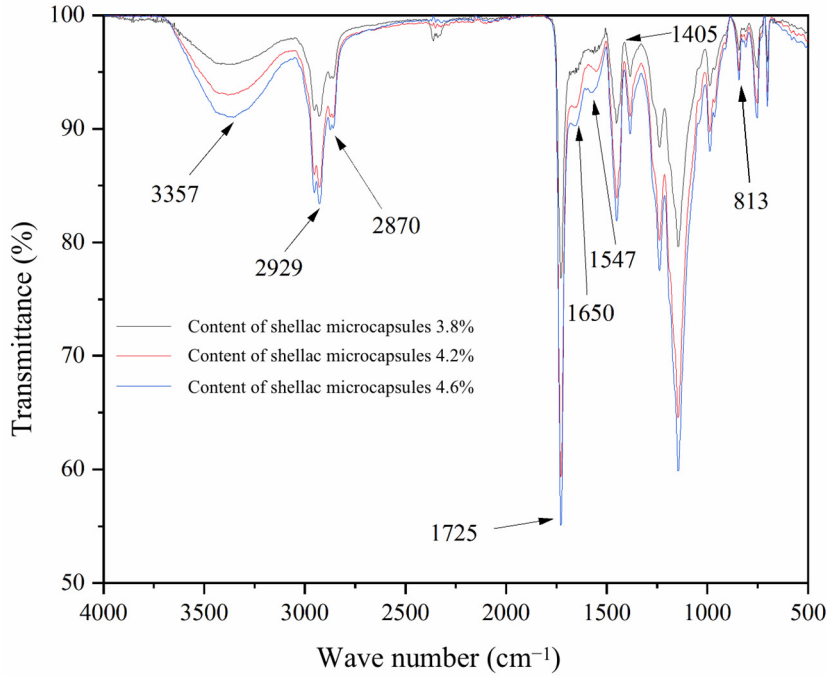

Figure 7. Infrared spectra of SCCBC with different shellac microcapsule contents.

3.8. Analysis of the Electromagnetic Wave Absorption Performance of Shellac Microcapsules, CIP, CNT Blended Powders

Based on the above analysis, it can be concluded that the SCCBC exhibits favorable overall performance when the content of shellac microcapsule is 4.2%. Therefore, the blended powder in the SCCBC corresponding to a microcapsule content of 4.2% was tested for its electromagnetic wave absorption performance. At this time, the shellac microcapsule content was 16%, the CIP content was 76.4%, and the CNTs content was 7.6%. Figures 8–10 show the absorption performance of the shellac microcapsules, CIP, CNT blended powders. Compared with the research by Zhou [39], it can be seen that shellac microcapsules, CIP, CNT blended powders have a certain electromagnetic wave absorption ability. From Figure 8, it can be seen that the real part of the dielectric constant e' of the shellac microcapsules, CIP, CNT blended powders shows a decreasing trend as a whole. The imaginary part e'' of the dielectric constant fluctuates around 9.0, which is probably caused by the dielectric polarization density and relaxation of the shellac microcapsules, CIP, CNT blended powders in this band, indicating that the shellac microcapsules, CIP, CNT blended powders have electrical loss characteristics. From Figure 9, it can be seen that the imaginary part of the magnetic permeability μ' gradually decreases when the frequency increases, indicating that the magnetic loss performance of the shellac microcapsules, CIP, CNT blended powders gradually weakens. However, all μ'' values are positive, indicating that the shellac microcapsules, CIP, CNT blended powders are absorbing radiation within this range. The shellac microcapsules, CIP, CNT blended powders achieved a theoretical minimum reflection loss of −7.94 dB at a matching thickness of 1.5 mm and 11.8 GHz, with a frequency band less than −5 dB ranging from 8.2 GHz to 17 GHz. From Figure 10, it can be seen that the electromagnetic wave absorption performance of shellac microcapsules, CIP, CNT blended powders in the low-frequency band is not good. This is because unmodified CIP itself has some defects. For example, at high frequencies, as the frequency increases, the magnetic permeability decreased, making it difficult to obtain relatively high magnetic permeability and meet the requirements of high electromagnetic wave absorption performance. Additionally, the CIP has a high density and poor antioxidant ability, which can reduce the electromagnetic wave absorption performance. Although adding CNTs can improve the density of CIP to some extent, the overall impedance matching is still poor.

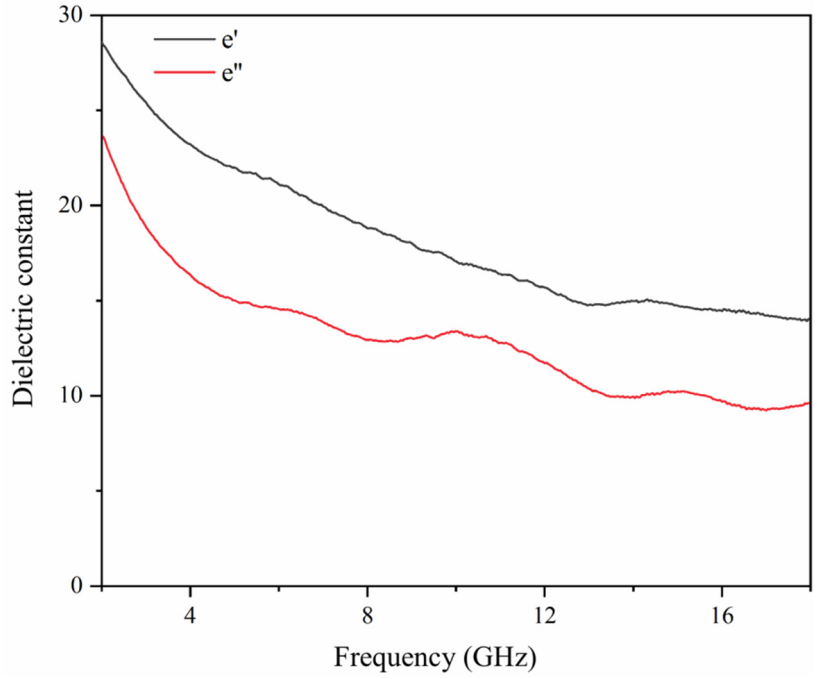

Figure 8. The dielectric constant of shellac microcapsules, CIP, CNT blended powders.

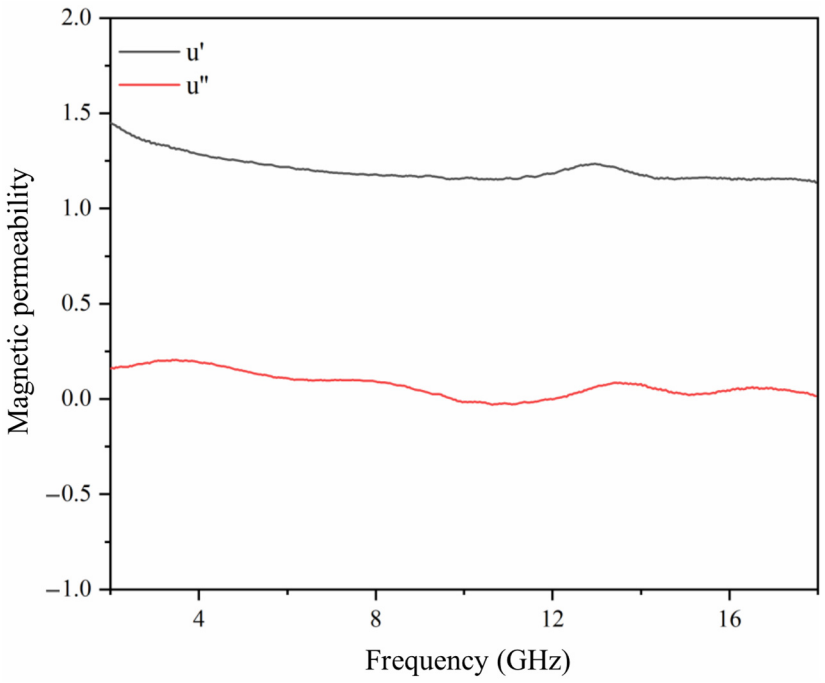

Figure 9. Magnetic permeability of shellac microcapsules, CIP, CNT blended powders.

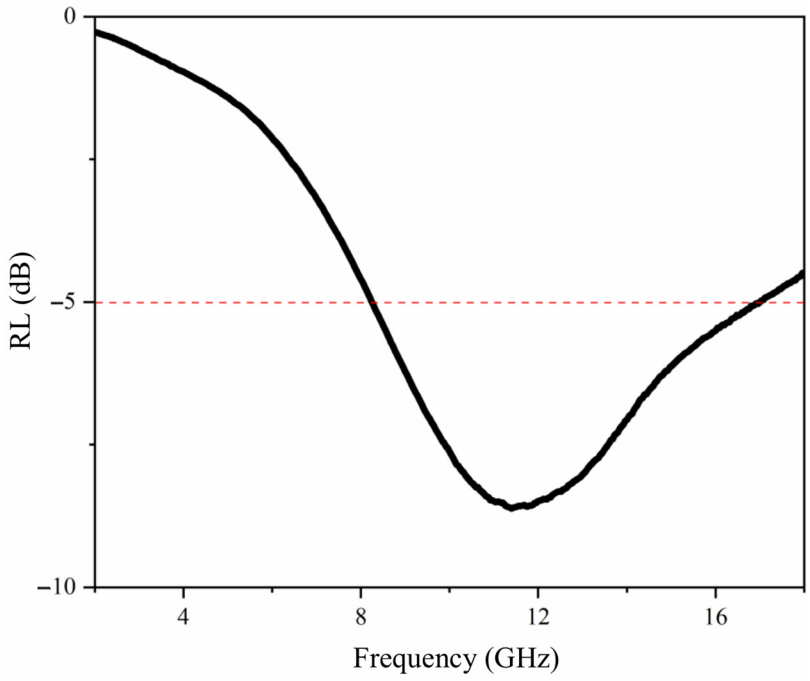

Figure 10. Theoretical reflection loss curve of shellac microcapsules, CIP, CNT blended powders (black line). The red dashed line represents the reference line for −5 dB.

4. Conclusions

The biggest factor affecting the elongation at tensile failure of the SCCBC is the shellac microcapsule content, followed by the content of CNTs, the CIP content and primer coating thickness. With an increase in microcapsule content, the color difference of SCCBC shows a gradual increment, the reason for this is as shellac microcapsule content gradually increases, the relative content of shellac microcapsules, CIP, CNT blended powders in waterborne primers increases, which is prone to aggregation and increases color difference. The glossiness decreases gradually with the increasing amount of shellac microcapsule content, this is because shellac microcapsules impact the surface smoothness and mirror reflection capability of the SCCBC, leading to a gradual reduction in glossiness as shellac microcapsule content rises. The increase in shellac microcapsule content gradually increases the adhesion level, hardness, and roughness of the SCCBC, the reason for this is the inclusion of powder in the primer. With a gradual rise in powder content, the coating experiences an increase in particulate matter. Consequently, this affects the adhesion capability between the coating and the wooden substrate, resulting in a raise in the adhesion level of the SCCBC. At the same time, the shellac microcapsules, CIP, CNT blended powders can fill the gaps and pores in the coating matrix. The addition of shellac microcapsules increases the solid content of coatings, thereby increasing the density of the SCCBC and gradually increasing the hardness of the SCCBC. The impact resistance, the elongation at tensile failure of the SCCBC and self-healing performance of SCCBC show a trend of increasing first and then decreasing, this is because adding shellac microcapsules can increase the hardness of the SCCBC, but excessive addition can lead to a decrease in the toughness of the SCCBC. Therefore, the cracks are prone to occur under external forces, resulting in a decrease in the impact resistance, the elongation at tensile failure of the SCCBC and self-healing performance of SCCBC. The SCCBC had a better liquid resistance to 75.0% ethanol solution, dishwashing liquid, and 15.0% NaCl solution, but a poor liquid resistance to red ink solution. The addition of shellac microcapsules, CIP, CNT blended powders did not alter the original chemical structure of the coating. When the shellac microcapsule content is 4.2%, CIP content is 20.0%, CIP/CNTs content is 2.0%, and the primer coating thickness is 25 μm, the comprehensive properties of the SCCBC is the best. In the meanwhile, the color difference of the SCCBC reaches 1.26, the glossiness at 60° incidence angle is 37.8 GU,

the adhesion is level 2, the hardness is 2H, the impact resistance is 15 kg·cm, and the roughness is 2.593 μm. The elongation at tensile failure of the SCCBC is 8.2%, and the self-healing rate is 24.1%. When the CIP content is 76.4%, CNTs content is 7.6%, and shellac microcapsule content is 16%, the theoretical minimum reflection loss is −7.94 dB at a matching coating thickness of 1.5 mm and frequency band of 11.8 GHz. The frequency band below −5 dB is 8.2–17 GHz. The experimental results provide a reference for the preparation of electromagnetic wave absorption and self-healing dual-function coatings on the surface of wooden materials.

Supplementary Materials: The following supporting information can be downloaded at: https://www.mdpi.com/article/10.3390/coatings13091572/s1, Table S1: Experimental materials; Table S2: List of experimental instruments.

Author Contributions: Conceptualization, methodology, validation, resources, data management, and supervision, Y.X.; formal analysis, investigation, X.Y.; and writing—review and editing, W.L. All authors have read and agreed to the published version of the manuscript.

Funding: This project was partly supported by the Natural Science Foundation of Jiangsu Province (BK20201386).

Institutional Review Board Statement: Not applicable.

Informed Consent Statement: Not applicable.

Data Availability Statement: Not applicable.

Conflicts of Interest: The authors declare that there is no conflict of interest.

References

1. Zhao, Z.N.; Niu, Y.T.; Chen, F.Y. Development and finishing technology of waterborne UV lacquer-coated wooden flooring. *Bioresources* **2021**, *16*, 1101–1114. [CrossRef]
2. Guan, T.; Du, Z.K.; Chang, X.Y.; Zhao, D.L.; Yang, S.R.; Sun, N.; Ren, B.Y. A reactive hydrophobically modified ethoxylated urethane (HEUR) associative polymer bearing benzophenone terminal groups: Synthesis, thickening and photo-initiating reactivity. *Polymers* **2019**, *178*, 121552. [CrossRef]
3. Feng, B.; Wang, D.; Li, Y.H.; Qian, J.P.; Yu, C.L.; Wang, M.S.; Luo, D.N.; Wei, S.Y. Mechanical properties of a soy protein isolate-grafted-acrylate (SGA) copolymer used for wood coatings. *Polymers* **2020**, *12*, 1137. [CrossRef]
4. Luo, Y.R.; Xu, W. Optimization of Panel Furniture Plates Rework Based on Intelligent Manufacturing. *Bioresources* **2023**, *18*, 5198–5208. [CrossRef]
5. Zhou, C.M.; Gu, W.H.; Luo, X.; Kaner, J. Building a 4E interview-grounded theory model: A case study of demand factors for customized furniture. *PLoS ONE* **2023**, *18*, 0282956. [CrossRef]
6. Guo, S.W.; Wang, D.; Shi, J.Y.; Li, X.; Feng, B.; Meng, L.L.; Cai, Z.Y.; Qiu, H.K.; Wei, S.Y. Study on waterborne acrylate coatings modified with biomass silicon. *Prog. Org. Coat.* **2020**, *135*, 601–607. [CrossRef]
7. Hao, W.F.; Hao, H.; Kanwal, H.; Jiang, S.P. Evaluation of Self-Healing Efficiency of Microcapsule-Based Self-Healing Cementitious Composites Based on Acoustic Emission. *J. Renew. Mater.* **2023**, *11*, 1687–1697. [CrossRef]
8. Wang, H.P.; Rong, M.Z.; Zhang, M.Q. Self-Healing Polymers and Polymer-Based Composites Containing Microcapsules. *Prog. Chem.* **2010**, *22*, 2397–2407.
9. Liu, Q.Q.; Gao, D.; Xu, W. Effect of Polyurethane Non-Transparent Coating Process on Coating Performance Applied on Modified Poplar. *Coatings* **2022**, *12*, 39. [CrossRef]
10. Jiang, S.P.; Lin, Z.Y.; Tang, C.; Hao, W.F. Preparation and Mechanical Properties of Microcapsule-Based Self-Healing Cementitious Composites. *Materials* **2021**, *14*, 4866. [CrossRef]
11. Ma, Y.X.; Liu, J.T.; Zhang, Y.R.; Ge, Y.; Wu, R.; Song, X.H.; Zhang, P.; Wu, J. Mechanical behavior and self-healing mechanism of polyurea-based double-walled microcapsule/epoxy composite films. *Prog. Org. Coat.* **2021**, *157*, 106283.
12. Qin, Y.Z.; Yan, X.X. Effect of the Addition of Shellac Self-Healing and Discoloration Microcapsules on the Performance of Coatings Applied on Ebiara Solid Board. *Coatings* **2022**, *12*, 1627.
13. Luo, Z.Y.; Xu, W.; Wu, S.S. Performances of Green Velvet Material (PLON) Used in Upholstered Furniture. *Bioresources* **2023**, *18*, 5108–5119. [CrossRef]
14. Han, Y.; Yan, X.X.; Tao, Y. Effect of Transparent, Purple, and Yellow Shellac Microcapsules on the Optical Properties and Self-Healing Performance of Waterborne Coatings. *Coatings* **2022**, *12*, 1056. [CrossRef]
15. Qu, Z.W.; Wang, Y.; Yang, P.A.; Zheng, W.; Li, N.; Bai, J.Y.; Zhang, Y.W.; Li, K.L.; Wang, D.S.; Liu, Z.H.; et al. Enhanced Electromagnetic Wave Absorption Properties of Ultrathin MnO_2 Nanosheet-Decorated Spherical Flower-Shaped Carbonyl Iron Powder. *Molecules* **2022**, *27*, 135.

16. He, Z.F.; Fang, Y.; Wang, X.J.; Pang, H. Microwave absorption properties of PANI/CIP/Fe_3O_4 composites. *Synth. Met.* **2011**, *161*, 420–425.
17. Yin, C.L.; Fan, J.M.; Bai, L.Y.; Ding, F.; Yuan, F.L. Microwave absorption and antioxidation properties of flaky carbonyl iron passivated with carbon dioxide. *J. Magn. Magn. Mater.* **2013**, *340*, 65–69.
18. Qiao, Y.J.; Yao, Z.D.; Li, Q.W.; Ji, Y.; Li, Z.N.; Zheng, T.; Zhang, X.H.; Wang, X.D. Preparation and microwave absorption of CIP/EP hollow spheres lattice composites. *Compos. Part A Appl. Sci. Manuf.* **2021**, *150*, 106626.
19. Chen, Q.L.; Li, L.Y.; Wang, Z.L.; Ge, Y.C.; Zhou, C.S.; Yi, J.H. Synthesis and enhanced microwave absorption performance of CIP@SiO_2@$Mn_{0.6}Zn_{0.4}Fe_2O_4$ ferrite composites. *J. Alloys Compd.* **2019**, *779*, 720–727. [CrossRef]
20. Zhou, J.J.; Wang, X.Y.; Ge, K.Y.; Yang, Z.Y.; Li, H.Q.; Guo, C.F.; Wang, J.Y.; Shan, Q.; Xia, L. Core-shell structured nanocomposites formed by silicon coated carbon nanotubes with anti-oxidation and electromagnetic wave absorption. *J. Colloid. Interf. Sci.* **2021**, *607*, 881–889.
21. Ding, X.W.; Lyu, L.F.; Wang, F.L.; Yang, Y.F.; Qiao, J.; Xu, D.M.; Zhang, X.; Kong, L.X.; Liu, J.R. Novel ternary Co_3O_4/CeO_2/CNTs composites for high-performance broadband electromagnetic wave absorption. *J. Alloys Compd.* **2021**, *864*, 158141.
22. Li, H.B.; Wu, W.H.; Hao, X.X.; Wang, S.; You, M.Y.; Han, X.Z.; Zhao, Q.; Xing, B.S. Removal of ciprofloxacin from aqueous solutions by ionic surfactant-modified carbon nanotubes. *Environ. Pollut.* **2018**, *243*, 206–217.
23. Deng, R.; Gao, X.; Hou, J.; Lin, D.H. Multi-omics analyses reveal molecular mechanisms for the antagonistic toxicity of carbon nanotubes and ciprofloxacin to *Escherichia coli*. *Sci. Total Environ.* **2020**, *726*, 138288. [PubMed]
24. Tao, Y.; Yan, X.X. Influence of HLB Value of Emulsifier on the Properties of Microcapsules and Self-Healing Properties of Waterborne Coatings. *Polymers* **2022**, *14*, 1304. [CrossRef]
25. Li, W.B.; Yan, X.X. Effects of Shellac Self-Repairing and Carbonyl Iron Powder Microcapsules on the Properties of Dulux Waterborne Coatings on Wood. *Polymers* **2023**, *15*, 2016.
26. Huang, Y.Y.; Wu, J. Preparation and Characterization of Graphene Oxide/Polyaniline/Carbonyl Iron Nanocomposites. *Materials* **2022**, *15*, 484.
27. Zhou, J.C.; Xu, W. Toward interface optimization of transparent wood with wood color and texture by silane coupling agent. *J. Mater. Sci.* **2022**, *57*, 5825–5838. [CrossRef]
28. Hu, W.G.; Yu, R.Z. Mechanical and acoustic characteristics of four wood species subjected to bending load. *Maderas-Cienc. Tecnol.* **2023**, *25*, 39.
29. Sun, H.M.; Shen, X.D.; Cui, S.; Xu, N. Preparation and absorption properties in near infrared wavelength of carbon nanotubes/acrylate coatings. *Chin. J. Chem. Eng.* **2007**, *20*, 784–788.
30. Li, R.R.; He, C.J.; Wang, X.D. Evaluation and modeling of processability of laser removal technique for bamboo outer layer. *JOM* **2021**, *73*, 2423–2430.
31. Li, R.R.; He, C.J.; Wang, X.D. Effects of processing parameters on mass loss and coating properties of poplar plywood during CO_2 laser modification. *Eur. J. Wood Wood Prod.* **2022**, *80*, 899–906. [CrossRef]
32. Sista, K.S.; Dwarapudi, S.; Kumar, D.; Sinha, G.R.; Moon, A.P. Carbonyl iron powders as absorption material for microwave interference shielding: A review. *J. Alloys Compd.* **2020**, *853*, 157251. [CrossRef]
33. Chang, Y.J.; Yan, X.X. Preparation and Self-Repairing Properties of MF-Coated Shellac Water-Based Microcapsules. *Coatings* **2022**, *10*, 778. [CrossRef]
34. Ataei, S.; Khorasani, S.N.; Torkaman, R.; Neisiany, R.E.; Koochaki, M.S. Self-healing performance of an epoxy coating containing microencapsulated alkyd resin based on coconut oil. *Prog. Org. Coat.* **2018**, *120*, 160–166. [CrossRef]
35. Wang, C.; Wang, J.; Niu, Y.G. Influence of phenolic resin surface treatment agent on interfacial adhesion of carbon fibre reinforced epoxy resin composites. *Adv. Compos. Lett.* **2007**, *16*, 237–241. [CrossRef]
36. Tezel, O.; Cigil, A.B.; Kahraman, M.V. Design and development of self-healing coating based on thiol-epoxy reactions. *React. Funct. Polym.* **2019**, *142*, 69–76. [CrossRef]
37. Liu, M.; Xu, G.L.; Wang, J.A.; Tu, X.W.; Liu, X.Y.; Wu, Z.H.; Lv, J.F.; Xu, W. Effects of Shellac Treatment on Wood Hygroscopicity, Dimensional Stability and Thermostability. *Coatings* **2020**, *10*, 881. [CrossRef]
38. Ni, X.; Luo, J.; Liu, R.; Liu, X.Y. A novel flexible UV-cured carbon nanotube composite film for humidity sensing. *Sens. Actuat. B-Chem.* **2019**, *297*, 126785. [CrossRef]
39. Zhou, M.; Gu, W.H.; Wang, G.H.; Zheng, J.; Pei, C.C.; Fan, F.Y.; Ji, G.B. Sustainable wood-based composites for microwave absorption and electromagnetic interference shielding. *J. Mater. Chem. A* **2020**, *8*, 24267–24283. [CrossRef]